



HAL
open science

Explicit Computations, Simulations and additional Results for the Dynamic Decentralized Control for Protocentric Aerial Manipulators

Marco Tognon, Burak Yüksel, Gabriele Buondonno, Antonio Franchi

► **To cite this version:**

Marco Tognon, Burak Yüksel, Gabriele Buondonno, Antonio Franchi. Explicit Computations, Simulations and additional Results for the Dynamic Decentralized Control for Protocentric Aerial Manipulators. [Research Report] Rapport LAAS n° 17048, LAAS-CNRS; Max Planck Institute for Biological Cybernetics; Sapienza Università di Roma. 2017. hal-01474695

HAL Id: hal-01474695

<https://hal.science/hal-01474695>

Submitted on 28 Feb 2017

HAL is a multi-disciplinary open access archive for the deposit and dissemination of scientific research documents, whether they are published or not. The documents may come from teaching and research institutions in France or abroad, or from public or private research centers.

L'archive ouverte pluridisciplinaire **HAL**, est destinée au dépôt et à la diffusion de documents scientifiques de niveau recherche, publiés ou non, émanant des établissements d'enseignement et de recherche français ou étrangers, des laboratoires publics ou privés.

Explicit Computations, Simulations and additional Results for the Dynamic Decentralized Control for Protocentric Aerial Manipulators

Technical Attachment to:

”Dynamic Decentralized Control for Protocentric Aerial Manipulators”
2017 IEEE International Conference on Robotics and Automation (ICRA),
Singapore, May 2017

Marco Tognon¹ Burak Yüksel² Gabriele Buondonno³ Antonio Franchi¹

INTRODUCTION

This document is a technical attachment to [1] for explicit computations of the nominal states and the inputs of a *Protocentric Aerial Manipulator* (PAM) in 2D, using differential flatness property. In [1] these values are used to control a PAM in 3D. Furthermore, considering the aerial manipulator design used for the experiments in that paper, here we investigate the case when the system is *non-protocentric*; i.e., the manipulating arm is not *exactly* attached to the CoM of the flying robot, P_0 . We show the effect of the distance between this attachment point and P_0 on the performance tracking a composite trajectory. Finally some additional plots related to the experimental results are provided.

A. Aerial physical interaction

For the reader interested in aerial vehicles physically interacting with the external environment, a rapidly expanding and broad topic, we also suggest the reading of [2], where a force nonlinear observer for aerial vehicles is proposed, of [3], where an IDA-PBC controller is used for modulating the physical interaction of aerial robots, of [4], [5] where fully actuated platforms for full wrench exertion are presented, of [6]–[8] where the capabilities of exerting forces with a tool are studied, and finally of [9]–[11] where aerial manipulators with elastic-joint arms are modeled and their controllability properties discovered. The reader interested in the analysis and control of tethered aerial vehicles (another form of physical interaction) is also referred to [12], where flatness, controllability and observability is studied, to [13] where the case of a moving

base is thoroughly analyzed, to [14] where real experiments for tethered landing on sloped surfaces is shown, and to [15], [16] where the case of multiple tethered vehicles is investigated.

I. EXPLICIT COMPUTATION OF THE NOMINAL STATES AND THE INPUTS

In Sec. IV of [1] we describe how the nominal states and the inputs of a PAM can be computed as sole functions of the flat outputs and their derivatives up to the fourth order. These flat outputs are given in the Fact. 1 of [1] as $\mathbf{y} = [\mathbf{p}_{0_{xz}}^T \mathbf{q}_r^T]^T \in \mathbb{R}^{(n+2)}$, where the generalized coordinates of the PAM in 2D is chosen as $\mathbf{q}_2 = [\mathbf{p}_{0_{xz}}^T \theta_0 \mathbf{q}_r^T]^T \in \mathbb{R}^{3+n}$ and the control inputs of the system are $\mathbf{u}_2 = [u_t \ u_r \ \boldsymbol{\tau}^T]^T \in \mathbb{R}^{2+n}$. This means that while the CoM positions of the VTOL and the absolute orientations of the links are direct functions of the flat outputs, \mathbf{y} , the computations of $\theta_0, \dot{\theta}_0$ (flying base pitch and its time derivatives), and $u_t, u_r, \tau_{\nu\mu}$ as functions of $\mathbf{y}, \dot{\mathbf{y}}, \ddot{\mathbf{y}}, \dddot{\mathbf{y}}$ are implicit.

Let us start with the computations of $\theta_0, \dot{\theta}_0$, and u_t . As it is given in (10) of the paper, these values are functions of the CoM position of the overall system, $\ddot{\mathbf{p}}_c$ and its derivative $\ddot{\mathbf{p}}_c$ (actually we also need to compute $\ddot{\mathbf{p}}_c$, because $\ddot{\theta}_0$ depends on it, and $\ddot{\theta}_0$ is needed for computing the torque u_r). Let us then compute the derivatives of \mathbf{p}_c . Taking the time derivatives of (11) of the paper (from second up to the fourth order), we have;

$$\begin{aligned} \ddot{\mathbf{p}}_c &= \frac{1}{m_s} \left(m_0 \ddot{\mathbf{p}}_{0_{xz}} + \sum_{j=1}^m \left(\sum_{i=1}^{n^j} (m_{ij} \ddot{\mathbf{p}}_{ij} + m_{m_{ij}} \ddot{\mathbf{p}}_{m_{ij}}) \right) \right) \\ \ddot{\mathbf{p}}_c &= \frac{1}{m_s} \left(m_0 \ddot{\mathbf{p}}_{0_{xz}} + \sum_{j=1}^m \left(\sum_{i=1}^{n^j} (m_{ij} \ddot{\mathbf{p}}_{ij} + m_{m_{ij}} \ddot{\mathbf{p}}_{m_{ij}}) \right) \right) \\ \ddot{\mathbf{p}}_c &= \frac{1}{m_s} \left(m_0 \ddot{\mathbf{p}}_{0_{xz}} + \sum_{j=1}^m \left(\sum_{i=1}^{n^j} (m_{ij} \ddot{\mathbf{p}}_{ij} + m_{m_{ij}} \ddot{\mathbf{p}}_{m_{ij}}) \right) \right). \end{aligned} \quad (1)$$

Now, for $\ddot{\mathbf{p}}_c, \ddot{\mathbf{p}}_c, \ddot{\mathbf{p}}_c$ to be functions of the flat outputs only we must show that $\ddot{\mathbf{p}}_{ij}, \ddot{\mathbf{p}}_{m_{ij}}, \ddot{\mathbf{p}}_{ij}, \ddot{\mathbf{p}}_{m_{ij}}, \ddot{\mathbf{p}}_{ij}, \ddot{\mathbf{p}}_{m_{ij}}$ can be computed using only the flat outputs and their derivatives.

¹LAAS-CNRS, Université de Toulouse, CNRS, Toulouse, France, antonio.franchi@laas.fr, marco.tognon@laas.fr

²Max Planck Institute for Biological Cybernetics, Spemanstr. 38, 72076, Tübingen, Germany, burak.yueksel@tuebingen.mpg.de

³Dipartimento di Ingegneria Informatica, Automatica e Gestionale, Sapienza Università di Roma, Via Ariosto 25, 00185 Roma, Italy, buondonno@diag.uniroma1.it

This work has been partially funded by the European Union’s Horizon 2020 research and innovation program under grant agreement No 644271 AEROARMS.

Flat outputs	From Fact 1 of [1], $\mathbf{y} = [\mathbf{p}_{0_{xz}}^T \mathbf{q}_r^T]^T \in \mathbb{R}^{2+n}$. Since $\exists f_e : \mathbf{p}_{0_{xz}} = f_e(\mathbf{p}_{e_{xz}} \mathbf{q}_r)$, it is also $\mathbf{y}_e = [\mathbf{p}_{e_{xz}}^T \mathbf{q}_r^T]^T \in \mathbb{R}^{2+n}$.
Nominal States	The variables $\mathbf{p}_{0_{xz}}$, $\dot{\mathbf{p}}_{0_{xz}}$, \mathbf{q}_r and $\dot{\mathbf{q}}_r$ are direct functions of \mathbf{y} and $\dot{\mathbf{y}}$. This leaves θ_0 and $\dot{\theta}_0$ to be computed. From (10) of [1], $\theta_0 = \theta_0(\bar{\mathbf{p}}_c)$. Hence from (1): $\bar{\mathbf{p}}_c = \bar{\mathbf{p}}_c(\bar{\mathbf{p}}_{0_{xz}}, \bar{\mathbf{p}}_{m_{\nu\mu}}, \bar{\mathbf{p}}_{\nu\mu})$, $\ddot{\mathbf{p}}_{m_{\nu\mu}} = \ddot{\mathbf{p}}_{m_{\nu\mu}}(\mathbf{y}, \dot{\mathbf{y}}, \ddot{\mathbf{y}})$, $\ddot{\mathbf{p}}_{\nu\mu} = \ddot{\mathbf{p}}_{\nu\mu}(\mathbf{y}, \dot{\mathbf{y}}, \ddot{\mathbf{y}}) \implies \bar{\mathbf{p}}_c = \bar{\mathbf{p}}_c(\mathbf{y}, \dot{\mathbf{y}}, \ddot{\mathbf{y}})$. Then $\theta_0 = \theta_0(\mathbf{y}, \dot{\mathbf{y}}, \ddot{\mathbf{y}})$. From (10) of [1], $\dot{\theta}_0 = \dot{\theta}_0(\bar{\mathbf{p}}_c, \dot{\bar{\mathbf{p}}}_c)$. Hence from (1): $\dot{\bar{\mathbf{p}}}_c = \dot{\bar{\mathbf{p}}}_c(\dot{\bar{\mathbf{p}}}_{0_{xz}}, \dot{\bar{\mathbf{p}}}_{m_{\nu\mu}}, \dot{\bar{\mathbf{p}}}_{\nu\mu})$, $\ddot{\mathbf{p}}_{m_{\nu\mu}} = \ddot{\mathbf{p}}_{m_{\nu\mu}}(\mathbf{y}, \dot{\mathbf{y}}, \ddot{\mathbf{y}})$, $\ddot{\mathbf{p}}_{\nu\mu} = \ddot{\mathbf{p}}_{\nu\mu}(\mathbf{y}, \dot{\mathbf{y}}, \ddot{\mathbf{y}}) \implies \dot{\bar{\mathbf{p}}}_c = \dot{\bar{\mathbf{p}}}_c(\mathbf{y}, \dot{\mathbf{y}}, \ddot{\mathbf{y}})$. Then $\dot{\theta}_0 = \dot{\theta}_0(\mathbf{y}, \dot{\mathbf{y}}, \ddot{\mathbf{y}})$.
Nominal Inputs	Considering (10) of [1] and $\bar{\mathbf{p}}_c$ from the above; first $u_t = u_t(\bar{\mathbf{p}}_c) \implies u_t = u_t(\mathbf{y}, \dot{\mathbf{y}}, \ddot{\mathbf{y}})$. Then, from [1], $\exists f_\tau : \tau_{\nu\mu} = \tau_{\nu\mu+1} + f_\tau(\bar{\mathbf{p}}_{0_{xz}}, \mathbf{q}_r, \dot{\mathbf{q}}_r, \ddot{\mathbf{q}}_r) \implies \tau_{\nu\mu} = \tau_{\nu\mu}(\mathbf{y}, \dot{\mathbf{y}}, \ddot{\mathbf{y}})$ where $\tau_{\nu\mu+1} = 0$ for $\nu\mu = n^\mu$. From (15) of [1], $u_r = J_0 \ddot{\theta}_0 + \sum_{j=1}^m \tau_{1j} - d_{G_x} u_t$. Above it is show that $u_t = u_t(\mathbf{y}, \dot{\mathbf{y}}, \ddot{\mathbf{y}})$, $\tau_{1\mu} = \tau_{1\mu}(\mathbf{y}, \dot{\mathbf{y}}, \ddot{\mathbf{y}})$, and from (10) of [1] it is $\ddot{\theta}_0 = \ddot{\theta}_0(\mathbf{y}, \dot{\mathbf{y}}, \ddot{\mathbf{y}}, \ddot{\mathbf{y}}, \ddot{\mathbf{y}})$. Then, $u_r = u_r(\mathbf{y}, \dot{\mathbf{y}}, \ddot{\mathbf{y}}, \ddot{\mathbf{y}}, \ddot{\mathbf{y}})$.

TABLE I: A summarizing table of the differential flatness of PAMs in 2D. Different outputs of the system are given on the top. The nominal states and inputs as implicit functions of the flat outputs and their derivatives up to the fourth order are provided. Note that for the ν^μ -th element of the system; $\mathbf{p}_{\nu\mu}$ and $\mathbf{p}_{m_{\nu\mu}}$ are the (time varying) individual link and motor CoM positions represented in \mathcal{F}_W , respectively.

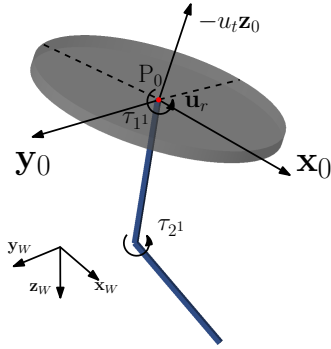


Fig. 1: A physical model of a PAM done in Sim Mechanics of Simulink–Matlab. The flying base is modeled as a cylindrical disk having the same mass and inertial parameters of our real VTOL system. Similar is done to the manipulating arm, consisting of two rigid bars. The actuation of the VTOL is done by applying $-u_t \mathbf{z}_0$ and \mathbf{u}_r at and around P_0 in 3D, respectively. Manipulating arms are actuated via velocity controlled motors.

For the ν -th motor of the μ -th manipulator (ν^μ -th motor of the system) it is:

$$\begin{aligned} \ddot{\mathbf{p}}_{m_{\nu\mu}}(\mathbf{y}, \dot{\mathbf{y}}, \ddot{\mathbf{y}}) &= \ddot{\mathbf{p}}_{0_{xz}} + \underbrace{\gamma_1(\mathbf{q}_{r^\mu}, \dot{\mathbf{q}}_{r^\mu}, \ddot{\mathbf{q}}_{r^\mu})}_{:=0, \text{ if } \nu^\mu=1} \\ \ddot{\mathbf{p}}_{m_{\nu\mu}}(\mathbf{y}, \dot{\mathbf{y}}, \ddot{\mathbf{y}}, \ddot{\mathbf{y}}) &= \ddot{\mathbf{p}}_{0_{xz}} + \underbrace{\gamma_2(\mathbf{q}_{r^\mu}, \dot{\mathbf{q}}_{r^\mu}, \ddot{\mathbf{q}}_{r^\mu}, \ddot{\mathbf{q}}_{r^\mu})}_{:=0, \text{ if } \nu^\mu=1} \\ \ddot{\mathbf{p}}_{m_{\nu\mu}}(\mathbf{y}, \dot{\mathbf{y}}, \ddot{\mathbf{y}}, \ddot{\mathbf{y}}, \ddot{\mathbf{y}}) &= \ddot{\mathbf{p}}_{0_{xz}} + \underbrace{\gamma_3(\mathbf{q}_{r^\mu}, \dot{\mathbf{q}}_{r^\mu}, \ddot{\mathbf{q}}_{r^\mu}, \ddot{\mathbf{q}}_{r^\mu}, \ddot{\mathbf{q}}_{r^\mu})}_{:=0, \text{ if } \nu^\mu=1}, \end{aligned} \quad (2)$$

where

$$\begin{aligned} \gamma_1 &= \sum_{i^\mu=1}^{\nu^\mu-1} \left(\bar{\mathbf{R}}_{0i^\mu} \bar{\mathbf{d}}_{i^\mu} \ddot{\theta}_{0i^\mu} - \mathbf{R}_{0i^\mu} \bar{\mathbf{d}}_{i^\mu} \dot{\theta}_{0i^\mu}^2 \right) \\ \gamma_2 &= \sum_{i^\mu=1}^{\nu^\mu-1} \left(\bar{\mathbf{R}}_{0i^\mu} \bar{\mathbf{d}}_{i^\mu} \ddot{\theta}_{0i^\mu} - 3\mathbf{R}_{0i^\mu} \bar{\mathbf{d}}_{i^\mu} \dot{\theta}_{0i^\mu} \ddot{\theta}_{0i^\mu} - \bar{\mathbf{R}}_{0i^\mu} \bar{\mathbf{d}}_{i^\mu} \dot{\theta}_{0i^\mu}^3 \right) \\ \gamma_3 &= \sum_{i^\mu=1}^{\nu^\mu-1} \left(\bar{\mathbf{R}}_{0i^\mu} \bar{\mathbf{d}}_{i^\mu} \ddot{\theta}_{0i^\mu} - 4\mathbf{R}_{0i^\mu} \bar{\mathbf{d}}_{i^\mu} \dot{\theta}_{0i^\mu} \ddot{\theta}_{0i^\mu} - \right. \\ &\quad \left. - 3\mathbf{R}_{0i^\mu} \bar{\mathbf{d}}_{i^\mu} \dot{\theta}_{0i^\mu}^2 - 6\bar{\mathbf{R}}_{0i^\mu} \bar{\mathbf{d}}_{i^\mu} \ddot{\theta}_{0i^\mu} \dot{\theta}_{0i^\mu}^2 + \mathbf{R}_{0i^\mu} \bar{\mathbf{d}}_{i^\mu} \dot{\theta}_{0i^\mu}^3 \right) \end{aligned}$$

with $\bar{\mathbf{d}}_* = \mathbf{d}_* + \tilde{\mathbf{d}}_*$ as defined in [1] and $\bar{\mathbf{R}}_* = \frac{\partial \mathbf{R}_*}{\partial \theta_*}$. This

gives the linear accelerations of the ν^μ -th motor CoM in the $\mathbf{x}_W - \mathbf{z}_W$ plane, and its first and second derivatives w.r.t. time as sole functions of the flat outputs. For the ν^μ -th link it is:

$$\begin{aligned} \ddot{\mathbf{p}}_{\nu\mu} &= \ddot{\mathbf{p}}_{m_{\nu\mu}} + \bar{\mathbf{R}}_{0\nu\mu} \mathbf{d}_{\nu\mu} \ddot{\theta}_{0\nu\mu} - \mathbf{R}_{0\nu\mu} \mathbf{d}_{\nu\mu} \dot{\theta}_{0\nu\mu}^2 \\ \ddot{\mathbf{p}}_{\nu\mu} &= \ddot{\mathbf{p}}_{m_{\nu\mu}} + \bar{\mathbf{R}}_{0\nu\mu} \mathbf{d}_{\nu\mu} \ddot{\theta}_{0\nu\mu} - \\ &\quad - 3\mathbf{R}_{0\nu\mu} \mathbf{d}_{\nu\mu} \dot{\theta}_{0\nu\mu} \ddot{\theta}_{0\nu\mu} - \bar{\mathbf{R}}_{0\nu\mu} \mathbf{d}_{\nu\mu} \dot{\theta}_{0\nu\mu}^3 \\ \ddot{\mathbf{p}}_{\nu\mu} &= \ddot{\mathbf{p}}_{m_{\nu\mu}} + \bar{\mathbf{R}}_{0\nu\mu} \mathbf{d}_{\nu\mu} \ddot{\theta}_{0\nu\mu} - 4\mathbf{R}_{0\nu\mu} \mathbf{d}_{\nu\mu} \dot{\theta}_{0\nu\mu} \ddot{\theta}_{0\nu\mu} - \\ &\quad - 3\mathbf{R}_{0\nu\mu} \mathbf{d}_{\nu\mu} \dot{\theta}_{0\nu\mu}^2 - 6\bar{\mathbf{R}}_{0\nu\mu} \mathbf{d}_{\nu\mu} \ddot{\theta}_{0\nu\mu} \dot{\theta}_{0\nu\mu}^2 + \mathbf{R}_{0\nu\mu} \mathbf{d}_{\nu\mu} \dot{\theta}_{0\nu\mu}^4. \end{aligned} \quad (3)$$

Using (2) in (3) we compute the linear acceleration of the ν^μ -th link CoM in the $\mathbf{x}_W - \mathbf{z}_W$ plane, and its first and second time derivatives as sole functions of the flat outputs. Substituting both (2) and (3) in (1) we do the same for the overall system CoM accelerations and its derivatives. Finally applying what derived so far to (10) in [1] and taking into account (9) in [1], we compute the nominal values of $\theta_0(\mathbf{y}, \dot{\mathbf{y}}, \ddot{\mathbf{y}})$, $\dot{\theta}_0(\mathbf{y}, \dot{\mathbf{y}}, \ddot{\mathbf{y}}, \ddot{\mathbf{y}})$, and $u_t(\mathbf{y}, \dot{\mathbf{y}}, \ddot{\mathbf{y}})$ as sole functions of the flat outputs and their finite number of derivatives.

The computation of u_r , $\tau_{\nu\mu}$, and hence τ are explained in [1]. Any further computation necessary to create the explicit mapping from the flat outputs to these inputs are already given in [10] and in [17]. A summary of these results is given in Table I.

II. EXTENSIVE SIMULATIONS

In [1], the experimental validation of the proposed controller using differential flatness is presented. The experimental setup consists of a Quadrotor VTOL and a two DoF manipulating arm (see Fig. 3 of the paper). The arm is attached to the quadrotor, with a 6[cm] of offset along the z -axis of \mathcal{F}_0 between the position of CoM of the VTOL (P_0) and the first joint. Despite this not being conform with the *protocentric* assumption of the design, performance degradation effects on the controller were not particularly noticeable.

This leads us to the question; what is the effect of the *non-protocentricity*, i.e., what if in the real system there is a generic offset between the CoM of the VTOL and the first joint of which the controller is not aware? An attempt to answer this

question is done in a simulation environment, using a physics-based model of our experimental setup built in *Sim-Mechanics* of Matlab–Simulink (see Fig. 1 for details).

Define $\mathbf{d}_0 = [d_{0_x} \ d_{0_z}]^T \in \mathbb{R}^2$ as the relative position between the attachment point of the first motor of the manipulating arm and P_0 expressed in \mathcal{F}_0 . We run a set of simulations testing the tracking of composite trajectories in the flat output space using the proposed controller, while varying the value \mathbf{d}_0 between the ranges

$$\begin{aligned} d_{0_x}^{min} &= 0 \text{ [m]}, \quad d_{0_x}^{max} = 0.4 \text{ [m]}, \\ d_{0_z}^{min} &= -0.4 \text{ [m]}, \quad d_{0_z}^{max} = 0.4 \text{ [m]} \end{aligned}$$

with a discrete sampling of 15 points. Thrust and torque limits of the quadrotor VTOL are also imposed (VTOL torque limits are chosen as ± 4.55 Nm; the minimum thrust is set to 1 [N] while maximum thrust is set to 21 [N]). The results are given in Fig. 2.

The initial condition is set far from the start of the desired trajectory in order to test the transient behavior. However from Fig. 2 it is clear that all the tracked outputs converge to their desired ones quickly. It is clearly shown that for the protocentric design, $\mathbf{d}_0 = \mathbf{0}$, the controller lets the system track the desired outputs almost perfectly. When the system is not protocentric ($\mathbf{d}_0 \neq \mathbf{0}$), then the outputs of the system start to diverge from the desired ones, which in turn forces the system actuators towards their limits. This is due to the dynamic effect of the non-protocentric design which is not considered in the controller, as well as the actuation limits that do not allow the feedback term of the controller to steer the system quickly to the desired values (see the last row of Fig. 1 for the control inputs). Nonetheless, the feedback term is still able to keep the real behavior close enough to the desired one, showing a good robustness, as explained in Sec. III of [1].

In the future, we plan to investigate the non-protocentric aerial manipulators and their control more in detail.

III. DETAILED EXPERIMENTAL RESULTS

In this section, and in particular in Figs 3, 4 and 5, we integrate the plots related to the experimental results presented in [1] with some additional informations, i.e., , the full state of the VTOL (position and orientation) and its thrust. The considerations and comments of the figures are the same of the ones in the paper.

REFERENCES

- [1] M. Tognon, B. Yüksel, G. Buondonno, and A. Franchi, “Dynamic decentralized control for protocentric aerial manipulators,” in *2017 IEEE Int. Conf. on Robotics and Automation*, Singapore, May. 2017.
- [2] B. Yüksel, C. Secchi, H. H. Bühlhoff, and A. Franchi, “A nonlinear force observer for quadrotors and application to physical interactive tasks,” in *2014 IEEE/ASME Int. Conf. on Advanced Intelligent Mechatronics*, Besançon, France, Jul. 2014, pp. 433–440.
- [3] —, “Reshaping the physical properties of a quadrotor through IDA-PBC and its application to aerial physical interaction,” in *2014 IEEE Int. Conf. on Robotics and Automation*, Hong Kong, China, May. 2014, pp. 6258–6265.
- [4] S. Rajappa, M. Ryll, H. H. Bühlhoff, and A. Franchi, “Modeling, control and design optimization for a fully-actuated hexarotor aerial vehicle with tilted propellers,” in *2015 IEEE Int. Conf. on Robotics and Automation*, Seattle, WA, May 2015, pp. 4006–4013.

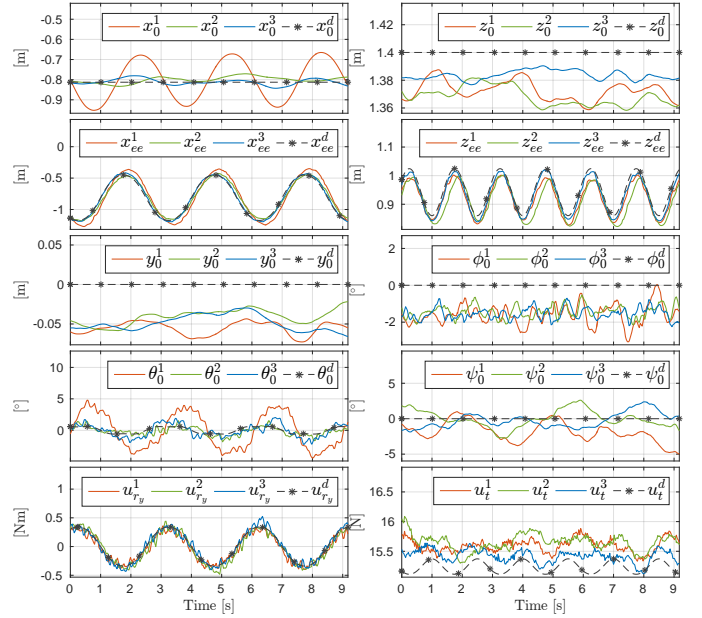


Fig. 3: Experimental results for trajectory (a).

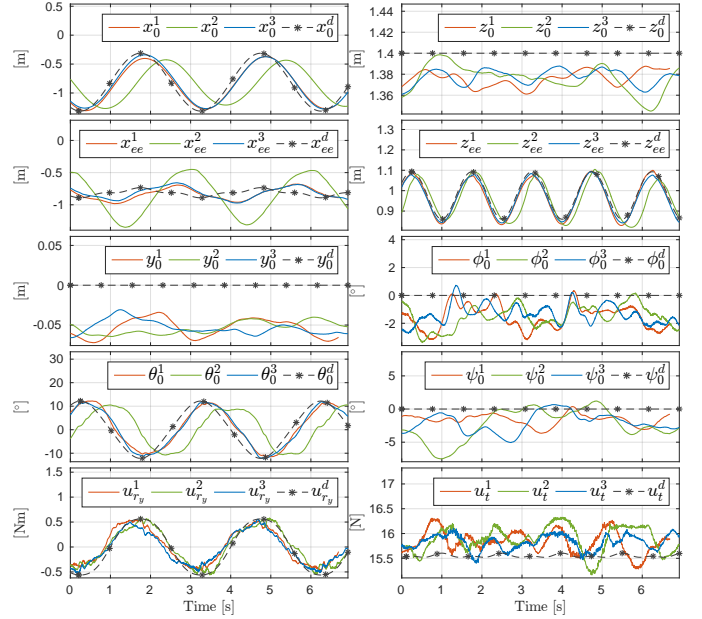


Fig. 4: Experimental results for trajectory (b).

- [5] M. Ryll, D. Bicego, and A. Franchi, “Modeling and control of FAST-Hex: a fully-actuated by synchronized-tilting hexarotor,” in *2016 IEEE/RSJ Int. Conf. on Intelligent Robots and Systems*, Daejeon, South Korea, Oct. 2016, pp. 1689–1694.
- [6] M. Mohammadi, A. Franchi, D. Barcelli, and D. Prattichizzo, “Cooperative aerial tele-manipulation with haptic feedback,” in *2016 IEEE/RSJ Int. Conf. on Intelligent Robots and Systems*, Daejeon, South Korea, Oct. 2016, pp. 5092–5098.
- [7] G. Gioioso, A. Franchi, G. Salvietti, S. Scheggi, and D. Prattichizzo, “The Flying Hand: a formation of uavs for cooperative aerial tele-manipulation,” in *2014 IEEE Int. Conf. on Robotics and Automation*, Hong Kong, China, May. 2014, pp. 4335–4341.
- [8] G. Gioioso, M. Mohammadi, A. Franchi, and D. Prattichizzo, “A force-based bilateral teleoperation framework for aerial robots in contact with the environment,” in *2015 IEEE Int. Conf. on Robotics and Automation*, Seattle, WA, May 2015, pp. 318–324.
- [9] B. Yüksel, N. Staub, and A. Franchi, “Aerial robots with rigid/elastic-joint arms: Single-joint controllability study and preliminary experiments,” in *2016 IEEE/RSJ Int. Conf. on Intelligent Robots and Systems*, Daejeon, South Korea, Oct. 2016, pp. 1667–1672.

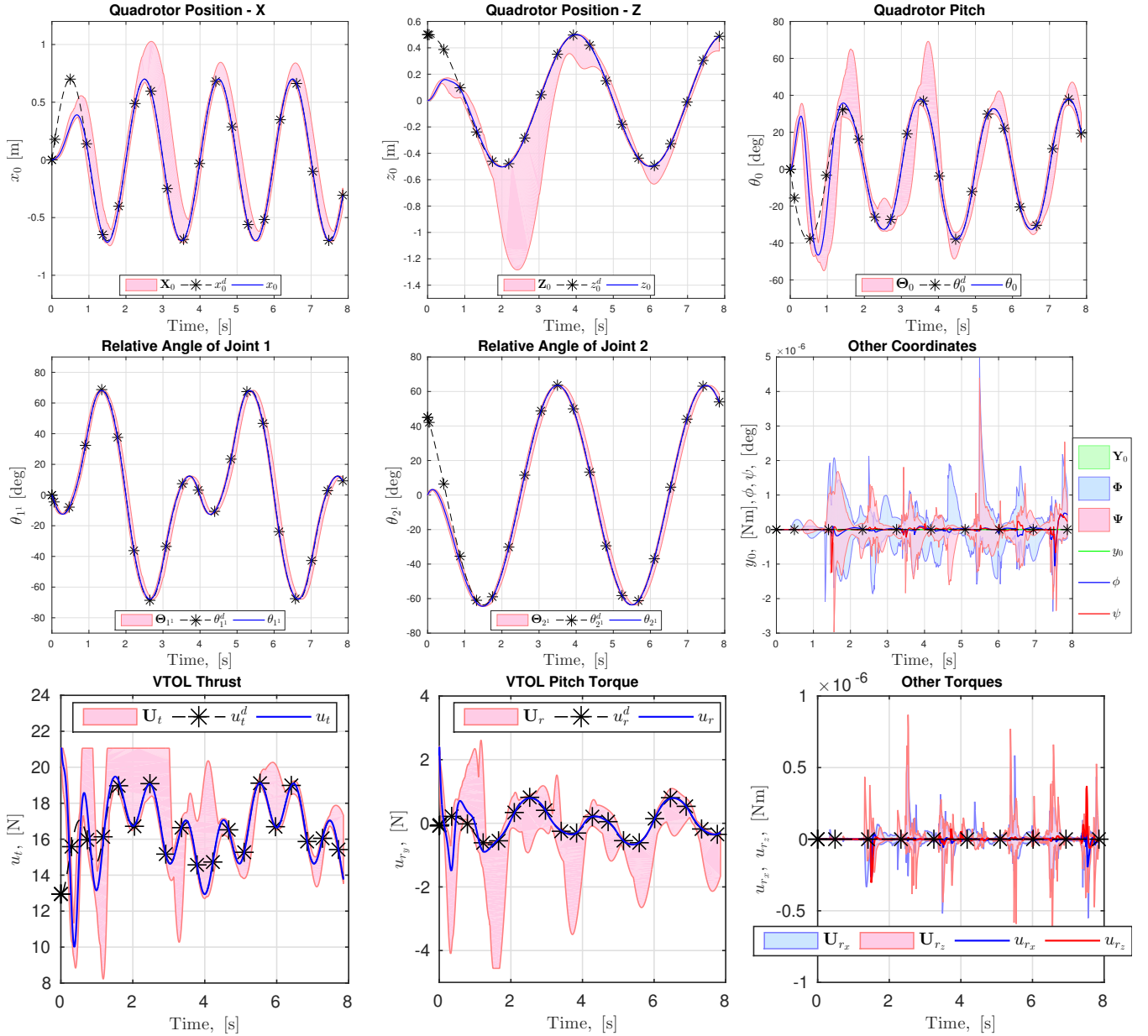


Fig. 2: Simulations for an aerial manipulator which is *not* proto-centric. The controller assumes the proto-centric design as presented in [1]. The coordinates in the plane of interest ($\mathbf{x}_W \times \mathbf{z}_W$) are shown in the first two columns, and all the other coordinates are gathered in the last row of the second column. The control inputs of the VTOL are given in the last row. The desired trajectories are depicted with black dashed curves. The blue solid curve used for the coordinates of the PAM when the model is proto-centric ($\mathbf{d}_0 = \mathbf{0}$). The red color is used to depict the evolution of the system with different non-proto-centric designs ($\mathbf{d}_0 \neq \mathbf{0}$): the maximum and the minimum values of all coordinates out of 15 simulations are plotted, and the space between them is filled in pink. A similar color code is used also for the control inputs. In the last sub-figures of the second and third rows, a different color code is used, but the same way of plotting is applied (notice that all values are almost zero). Notice the transient phase at the beginning of the simulations.

- [10] B. Yüksel, G. Buondonno, and A. Franchi, “Differential flatness and control of proto-centric aerial manipulators with any number of arms and mixed rigid-/elastic-joints,” in *2016 IEEE/RSSJ Int. Conf. on Intelligent Robots and Systems*, Daejeon, South Korea, Oct. 2016, pp. 561–566.
- [11] B. Yüksel, S. Mahboubi, C. Secchi, H. H. Bühlhoff, and A. Franchi, “Design, identification and experimental testing of a light-weight flexible-joint arm for aerial physical interaction,” in *2015 IEEE Int. Conf. on Robotics and Automation*, Seattle, WA, May 2015, pp. 870–876.
- [12] M. Tognon and A. Franchi, “Dynamics, control, and estimation for aerial robots tethered by cables or bars,” *IEEE Trans. on Robotics*, 2017.
- [13] M. Tognon, S. S. Dash, and A. Franchi, “Observer-based control of position and tension for an aerial robot tethered to a moving platform,” *IEEE Robotics and Automation Letters*, vol. 1, no. 2, pp. 732–737, 2016.
- [14] M. Tognon, A. Testa, E. Rossi, and A. Franchi, “Takeoff and landing on slopes via inclined hovering with a tethered aerial robot,” in *2016 IEEE/RSSJ Int. Conf. on Intelligent Robots and Systems*, Daejeon, South Korea, Oct. 2016, pp. 1702–1707.
- [15] M. Tognon and A. Franchi, “Control of motion and internal stresses for a chain of two underactuated aerial robots,” in *14th European Control Conference*, Linz, Austria, Jul. 2015, pp. 1620–1625.
- [16] —, “Nonlinear observer for the control of bi-tethered multi aerial robots,” in *2015 IEEE/RSSJ Int. Conf. on Intelligent Robots and Systems*, Hamburg, Germany, Sep. 2015, pp. 1852–1857.
- [17] B. Yüksel, G. Buondonno, and A. Franchi, “Proto-centric aerial manipulators: Flatness proofs and simulations,” LAAS-CNRS, Tech. Rep. hal-01351153, July 2016. [Online]. Available: <https://hal.archives-ouvertes.fr/hal-01351153>

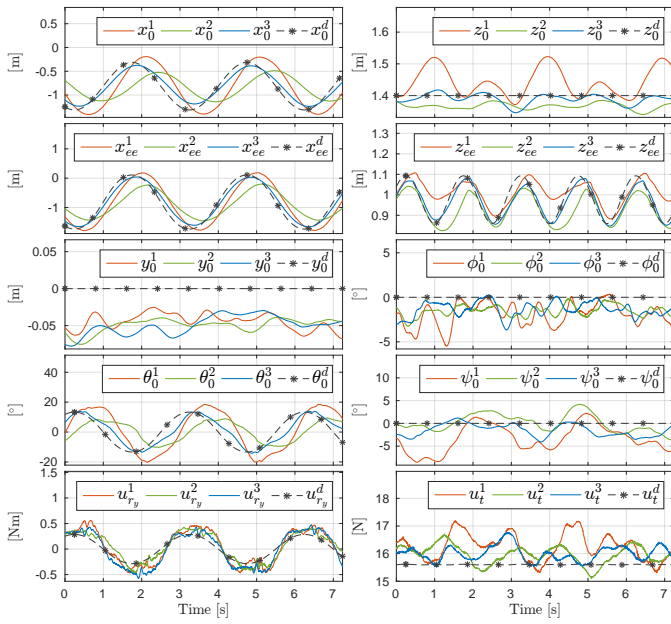


Fig. 5: Experimental results for trajectory (c).